2006 International Joint Conference on Neural Networks
Sheraton Vancouver Wall Centre Hotel, Vancouver, BC, Canada
July 16-21, 2006

# Classifying Single-Trial ERPs from Visual and Frontal Cortex during Free Viewing

Akaysha C. Tang, Matthew T. Sutherland, Christopher J. McKinney, Jing-Yu Liu, Yan Wang, Lucas C. Parra, Adam D. Gerson, and Paul Sajda

*Abstract*—**Event-related potentials (ERPs) recorded at the scalp are indicators of brain activity associated with event-related information processing; hence they may be suitable for the assessment of changes in cognitive processing load. While the measurement of ERPs in a laboratory setting and classifying those ERPs is trivial, such a task presents major challenges in a "real world" setting where the EEG signals are recorded when subjects freely move their eyes and the sensory inputs are continuously, as opposed to discretely presented. Here we demonstrate that with the aid of second-order blind identification (SOBI), a blind source separation (BSS) algorithm: (1) we can extract ERPs from such challenging data sets; (2) we were able to obtain meaningful single-trial ERPs in addition to averaged ERPs; and (3) we were able to estimate the spatial origins of these ERPs. Finally, using back-propagation neural networks as classifiers, we show that these single-trial ERPs from specific brain regions can be used to determine moment-to-moment changes in cognitive processing load during a complex "real world" task.**

## I. INTRODUCTION

Laboratory-based brain research typically imposes various constraints on the stimuli used to evoke brain responses as well as on the experimental subjects. In an electroencephalographic (EEG) study, discrete visual stimuli are typically presented with explicit onset and offset. This explicit stimulus onset allows signal averaging over many trials of repeated presentation whereby improving the signal-to-noise ratio of the resulting averaged event-related potentials (ERPs). Subjects are often asked to fixate their eyes at a particular point on the display sometimes with head stabilization through the use of a chin rest or a bite bar. These constraints ensure that repeated visual stimulations are as identical as possible. Furthermore, a subject may be asked to avoid or minimize eye blink, a major source of artifact that can contaminate ERP data, during EEG data acquisition. As eye blinks, eye movements, and head movements are unavoidable, researchers typically reject data trials that are contaminated by such artifacts before their analysis of the ERPs. Data rejection rates are highly variable and are permitted to be as high as 1/3 of the total data trials collected [1]. Because these constraints appear to be necessary for obtaining quality ERP data, few ERP researchers have attempted to investigate psychological functions under "natural" conditions, particularly with continuous (non-discrete) visual stimulation and free-eye movement.

Adding to this difficulty of studying brain functions under natural conditions is a more general issue concerning the nature of EEG signals. The scalp-recorded EEG data are mixtures of electrical signals arising from multiple regions of the brain as well as various artifacts related to eye-movement, blinking, muscle activity, line noise, and others. Therefore, the spatial origin of signals recorded at the scalp is not necessarily immediately underneath those sensors. In order to make statements about signals arising from specific brain regions one needs to solve the inverse problem of localizing each of the source signals from their mixtures. Although the inverse problem has no unique solution, blind source separation (BSS) and independent component analysis (ICA) algorithms [2]-[6] can be used to "reduce" the inverse problem by decomposing the mixture of signals into functionally distinct components. Some of these components can be localized with significantly reduced uncertainty. For example, a subset of the components recovered by BSS correspond to ocular artifacts, muscle activity, and sensor noise [7]-[11], and more importantly others correspond to neuronal signals originating from specific regions of the brain [3], [4], [6], [9], [10]. The ERPs generated from these neuronal component signals differ from ERPs generated from the mixtures of signals measured by the EEG sensors in that the former typically have a focal spatial origin corresponding to functionally unique brain regions while the spatial origin of the latter is not clearly defined due to the mixed nature of the signals.

Second-order blind identification (SOBI [12]) is a unique BSS algorithm that can separate functionally distinct but correlated brain activity [10], [13] as well as isolate ocular artifacts and sensor noise from brain signals [10], [11], [14]. In the present study, we apply SOBI to a challenging EEG data set collected during the performance of a task which involves continuously changing visual information and

This work was supported by a DARPA grant from the Augmented Cognition Program (ONR: N00014-02-1-0348) and the MIND institute (#2021) to ACT.

A. C. Tang is with the University of New Mexico, Departments of Psychology, and Neurosciences, Albuquerque, NM 87131 USA (phone: 505-610-9077; fax: 505-277-1394; email: akaysha@unm.edu).

M. T. Sutherland and C.J. McKinney are with the University of New Mexico, Department of Psychology, Albuquerque, NM 87131 USA.

J.Y. Liu and Y. Wang are with the University of New Mexico, Department of Electrical and Computer Engineering, Albuquerque, NM 87131 USA.

L.C. Parra is with the City College of New York, Department of Biomedical Engineering, New York, NY 10031 USA.

A.D. Gerson and P. Sajda are with Columbia University, Department of Biomedical Engineering, New York, NY 10027 USA.

0-7803-9490-9/06/$20.00/©2006 IEEE

requires continuous free-eye movements. This task involved 15 min of video game play under varying difficulty levels. We show that extraction of single-trial ERPs from *specific brain regions* is possible even under these challenging conditions. Previously, SOBI pre-processing has been shown to improve single-trial classification ability for data obtained under laboratory conditions [15], [16]. Here, we demonstrate that single-trial ERPs from SOBI-recovered neuronal components can be used to classify brief moments of high and low cognitive processing load during a real world task.

## II. Methods

### A. Behavioral Task

Three subjects performed a computer-simulated naval command control task, the Warship Commander Task [17] in an electrically noisy office environment. This task involves the presentation of a continuous stream of visual information, free-eye movements, lack of fixation points, and normal hand, arm, shoulder, and head movements. The operator's goal is to defend an aircraft carrier by shooting down as many enemy planes as possible while avoiding firing upon friendly planes. This task engages several types of highly inter-mixed cognitive processes: visual detection, spatial divided attention, tracking of moving targets, spatial working memory for previously identified planes, verbal working memory for an identified plane under inquiry, and language processing when reading displayed verbal messages.

We focused our analysis on two contrasting task-related events: a high and a low cognitive load event. The high load event is the COMM event which corresponds to the pressing of one of the many communication channel buttons. This event is preceded by remembering the communication channel number of a selected flight while simultaneously tracking and attending previously identified enemy planes, and is followed by a lateral eye movement to the message display box and reading of a verbal message which indicates whether the currently selected plane is friendly or hostile. Thus, surrounding a COMM event, the operator is engaged in several types of higher level cognitive processing. In contrast, a WARN event corresponds to the pressing of the WARN button. This event is preceded by selection of an already identified enemy plane and followed by a 3 sec waiting period before the enemy can be fired upon. Thus, the WARN event requires much less cognitive processing than the COMM event. These two events are intermixed with each other and embedded among many other ongoing events that potentially attract the operator's attention (Fig. 1).

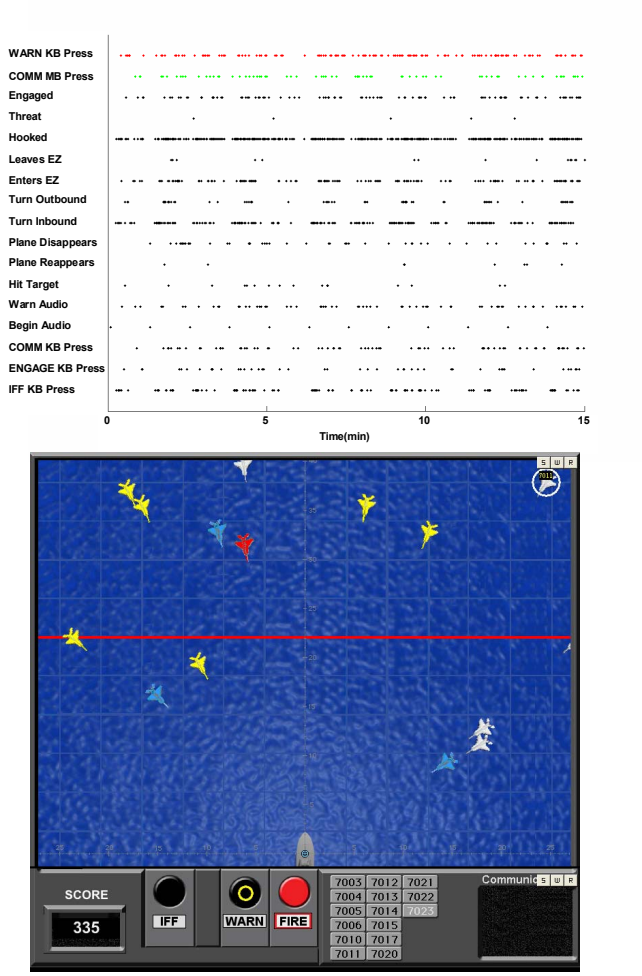


Fig. 1. (Top) Events during 15 min of game play. Red: WARN events; Green: COMM events; black: other unanalyzed events. (Bottom) The Warship Commander Task display window. From right to left: message display box; communication channels; fire button; and warn button.

### B. EEG Signal Processing

We collected 64 channel EEG data (sampling rate: 500Hz; bandpass filter: 1-100Hz; 15 min duration). The 64 channel EEG data was decomposed into 64 SOBI components. Task related components were further identified temporally using event triggered averages and spatially using a commercially available source modeling, Package (BESA 5.0, Brain Electrical Source Analysis; MEGIS Software; Munich, Germany). For the most recent detailed descriptions of this source identification process, see [10], [13], [16].

Details on SOBI [12] as well as its application to EEG/MEG data [6], [9], [11], [13], [15] have been described elsewhere. A brief step-by-step description is provided here as a flow chart (Fig. 2). SOBI decomposes $n$-channel continuous EEG data into $n$ components (Step 1, Fig. 2), each of which corresponds to a recovered putative source that contributes to the scalp recorded EEG signals. Each SOBI component has an associated time course of activation and a sensor space projection (scalp map) that specifies the effect of that component, in isolation, on each of the $n$ electrodes. Let $\mathbf{x}(t)$ represent the $n$ continuous time series from the $n$ EEG channels, where $\mathbf{x}_i(t)$ corresponds to the $i^{th}$

EEG channel. Because various underlying sources are summed via volume conduction to give rise to the scalp EEG, each of the $\mathbf{x}_i(t)$ is assumed to be an instantaneous linear mixture of $n$ unknown components or sources $\mathbf{s}_i(t)$, via an unknown $n \times n$ mixing matrix **A,**

$$\mathbf{x}(t) = \mathbf{A}\mathbf{s}(t).$$

The putative sources, $\hat{\mathbf{s}}(t)$, are given by,

$$\hat{\mathbf{s}}(t) = \mathbf{W}\mathbf{x}(t),$$

where,

$$\mathbf{W} = \mathbf{A}^{-1}.$$

SOBI finds the unmixing matrix **W** through an iterative process that minimizes the sum squared cross-correlations between one recovered component at time t and another at time t + $\tau$, across a set of time delays [18]. The following set of delays, $\tau$s (in ms), were chosen to cover a reasonably wide interval without extending beyond the support of the autocorrelation function:

$\tau \in$ {1, 2, 3, 4, 5, 6, 7, 8, 9,
13, 15, 18, 20, 23, 25, 28, 30, 33, 35, 38, 40, 43, 45, 48,
50, 60, 70, 80, 90, 100, 110, 120, 130, 140, 150, 160,
170, 180, 190, 200, 210, 220, 230, 240, 250}.

Similar sets of $\tau$s have been used to effectively isolate artifacts from EEG and MEG data as well as various task-related neuronal components [9], [10], [16]. For details on how the choice of time delay parameters affect the extraction of SI signals see [13].

The time course of the $i^{th}$ component is given by $\hat{\mathbf{s}}_i(t)$, from which ERPs for each recovered component can be generated (Step 2, Fig. 2). Components whose ERPs displayed activation following the COMM or WARN events were conservatively identified as potential components of interest. ERPs were generated for both the COMM and WARN events.

The spatial location of the $i^{th}$ component is determined by the $i^{th}$ column of $\hat{\mathbf{A}}$ (referred to as the component's sensor weights) (Step 3, Fig. 2), $\hat{\mathbf{A}} = \mathbf{W}^{-1}$. By assessing the sensor weights of a component, candidate neuronal components or known artifact components can be identified. For example, a visual component may have large and focally distributed sensor weights over posterior regions of the scalp and an ocular component will show large weights for sensor locations near the eyes (see end product of Step 3 in Fig. 2).

From the above two independently constructed candidate component lists, an overlapping set of components were further evaluated (Step 4, Fig. 2). The signal strength of the $i^{th}$ component, measured across all sensors at time t in the original units of measure (here $\mu V$), can be estimated from its sensor space projection $\hat{\mathbf{x}}^{(i)}(t)$,

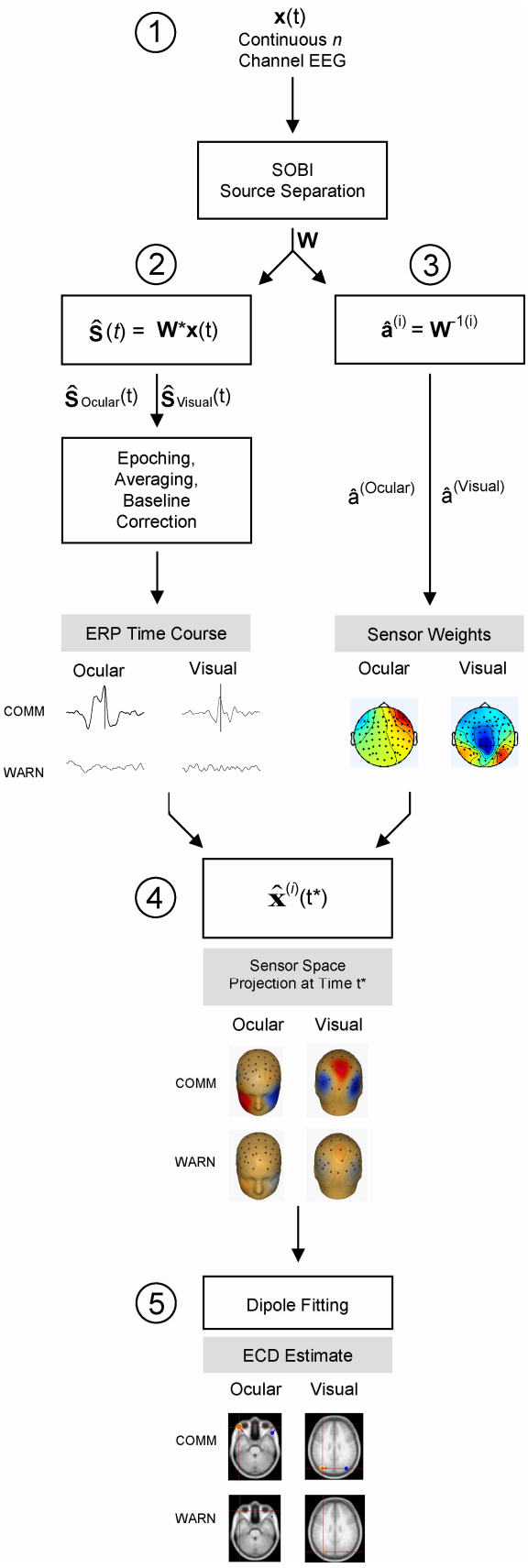


Fig. 2. Schematic illustration of SOBI-aided extraction of neuronal and artifactual components. An ocular and visual component are used as examples of $\hat{\mathbf{s}}_i$ for illustrative purposes.

$$\hat{\mathbf{x}}^{(i)}(t) = \hat{\mathbf{s}}_i(t)\hat{\mathbf{a}}^{(i)},$$

where $\hat{\mathbf{a}}^{(i)}$ is the $i^{th}$ column of $\hat{\mathbf{A}}$, i.e. the sensor weights, and $\hat{\mathbf{s}}_i(t)$ is a scalar. A candidate's averaged ERP following COMM or WARN events can then be projected at each of the sensors as 3-D scalp current source density (CSD) maps, which are the second spatial derivative of the voltage distribution and are considered better at visually revealing the underlying source generators than the potential maps themselves [19].

The components' locations were then estimated from the sensor space projections (Step 5, Fig. 2) using BESA. Equivalent current dipoles (ECDs) were fit for the small set of candidate components with an ellipsoidal four-shell head model fit for each subject using their digitized electrode positions. ECD locations (mm) were found using a least-squares algorithm at the peak time of the corresponding average ERP (t*). Note that the sensor space projections can be used as input not only to point-source modeling algorithms e.g. [20], [21] but distributed-source modeling methods as well e.g. [22], [23].

In contrast to typically how BESA is used for source modeling, here the input data to BESA was the ERP sensor space projections of a single SOBI-recovered component, as opposed to the original EEG sensor readings. The former is viewed as containing signals from a functionally distinct neuronal population while the latter containing electrical signals from many neuronal as well as noise sources. Because a SOBI component has a fixed sensor space projection, $\hat{\mathbf{a}}^{(i)}$, the estimated dipole location does not change with respect to time. In contrast, when fitting multiple dipole sources from the mixture of EEG signals, one must consider the fact that each underlying source can have a different time course of activation, thus their mixing changes over time. Consequently, the estimated dipole locations may also change when fit at different times and somewhat arbitrary decisions must be made. Choosing which of these multiple alternatives to report requires significant subjectivity. Here, by taking a SOBI component as the starting point for source localization, complications regarding the time of model fitting were circumvented.

### C. Back-Propagation Neural Networks (BPNNs)

Two major advantages that SOBI components offer is improved signal-to-noise ratio in both the component's average and single-trial ERPs [10], [13], [15] and increased certainty in the component's spatial origin [9], [10]. With these improved capabilities, we hoped to determine whether the neuronal activity from a set of specific functionally distinct brain regions could tell us about the processing load of an individual. To do so single-trial ERPs from two SOBI-recovered components (see section III C,D) time-locked to the WARN and COMM events were used as input to BPNNs. ERP researchers typically perform their analyses after rejecting data from trials that are contaminated by various artifacts. Because the present task requires continuous free-eye movement, the typical data exclusion method would be inappropriate here. Instead, using SOBI, artifactual signals are isolated and separated into distinct components without the need to discard trials containing such artifacts. Thus all events in the data set were classified without exclusion.

We trained three-layer networks to classify two event types: WARN and COMM, using single-trial ERPs generated around these two events. The WARN events entail relatively low processing load and the COMM events high processing load. The input time window for each component is 700 ms long (from 100 ms before to 600 ms after the event). At the sampling rate of 500 Hz, a total of 350 data points (500 samples * 700 ms / 1000 ms) were within this range. To reduce noise, for each SOBI component the single-trial ERP data were further smoothed and reduced to 35 averages (10 data points per average). As two SOBI components were used for classification, a total of 70 (2 x 35) inputs units were used. The same number of hidden units (70) was used. Increasing the number of hidden units or hidden layers did not significantly affect the results of classification (data not shown).

To train the network, the traingdx learning algorithm (Matlab Neural Network Toolbox, MathWorks, Inc., Natick, MA) was employed, which uses gradient descent with momentum and variable learning rate in batch learning mode [24]. While gradient descend with momentum can avoid a shallow local minimum, a variable learning rate can make the learning as fast as possible while maintaining stability. The batch-learning mode was used to update the network weights after all training data were presented.

We assessed classification performance by comparing the ability of a trained network classifier to generalize from one subset of data (training set) to another (test set). After a network was trained with 50% of the data (training set, randomly selected) to 95% classification accuracy, the generalization performance of the trained network was then evaluated using the remaining 50% of the data (test data). To properly estimate classification accuracy, this training-testing process was repeated 100 times, each time using a different randomly selected pair of training-testing datasets along with a different set of random starting weights at the beginning of training (i.e. 100 x cross-validation).

## III. Results

### A. Isolation of Various Artifacts

When a subject is engaged in tasks like video game play, small head and arm movements are unavoidable. Therefore, movement related artifacts were present throughout the data. Additionally, from the scalp projections, sensor artifact-related components can be identified by their focal activations. These components' sensor projections were best fitted by ECDs located on the surface of the skull, indicating their origin at or near the scalp (Fig. 3, top panels). As the

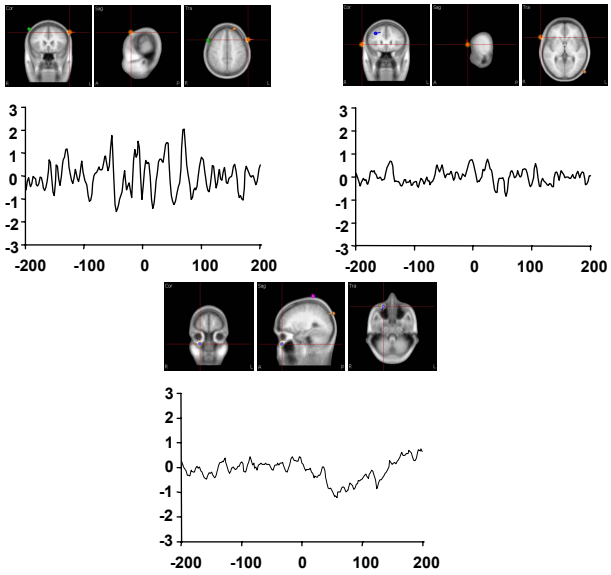


Fig. 3. Three examples of SOBI noise-components. ECDs are superimposed on a standard structural MRI and single epochs are shown.

amplitude of these noise sources at the scalp was as large as a few microvolts (Fig. 3, bottom panels), isolation of such noise components is critical for improving the signal-to-noise ratio of neuronal components of interest.

### *B. Isolation of Eye-Movement Related Signals*

To perform the task, the operator must continuously monitor and track a large number of inbound planes as well as read and interpret various control button labels and displays. Therefore, continuous eye movement is an integral part of task performance which highly overlaps with cognitive processing. Rejecting such artifacts by removing data, as may be done in a more conventional approach, would defeat the purpose of the study. Three types of ocular components (blink, vertical, and lateral movement) were reliably recovered by SOBI (data not shown). Figure 4 shows a SOBI-component corresponding to lateral eye movement. This component can be fit by a pair of symmetric ECDs located near the eyes with above 95% goodness-of-fit (Fig 4B). The COMM event-triggered average from this component is similar to that obtained when the subject was instructed to make controlled lateral eye movements before the experiment began (data not shown). The ERP waveform in Figure 4C shows two separate horizontal eye movement related deflections. The first large amplitude change can be seen starting prior to the COMM event (0 ms), which reflects the oblique eye movement from a location on the screen to the communication buttons, and a second change occurs when a horizontal eye movement was made from the COMM button to the display box at the lower-right corner (see Fig. 1). In contrast, during WARN events, the subject did not have to make any consistent horizontal eye movement. This is reflected by the lack of activity in the ERPs generated around the WARN events (Fig. 4D). The

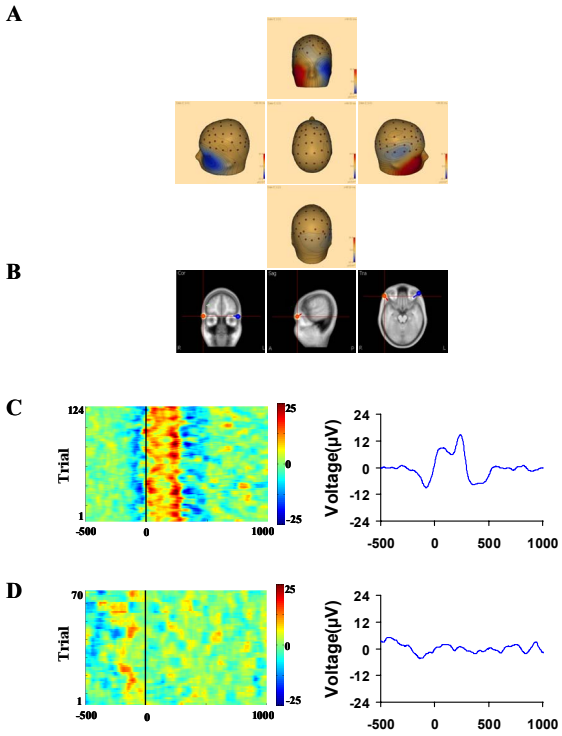


Fig. 4. An ocular SOBI component reflecting lateral movement. (A) CSD scalp map. (B) ECD model. (CD-left) single-trial ERP display. (CD-right) averaged ERP. (C) COMM events. (D) WARN events.

isolation of this large amplitude artifact is particularly important for unmasking the relatively weaker neuronal signals.

### *C. Isolation of Neuronal Activity Related to Early Visual Processing*

In contrast to typical experiments involving visual stimuli, the Warship Commander Task requires visual processing under "natural" vision. In addition to free-eye movement and continuously presented information, the visual processing is particularly demanding as it involves intermixed and rapid discrimination and tracking of moving targets in different colors, reading of labels and text, divided visual attention among multiple moving targets, working memory, and visually based rapid decision making. We show that a SOBI visual component can be extracted from EEG data collected under such conditions. Figure 5 shows a SOBI component whose sensor projection (Fig. 5A) can be fitted with a pair of symmetric dipoles located in visual cortex with over 90% goodness-of-fit (Fig. 5B). When the single-trial (Fig. 5C, left) and averaged ERPs (Fig. 5C, right) were time-locked to COMM button presses, the resulting evoked potentials resembled a visual evoked potential (VEP) recorded under ideal experimental conditions. Together, the spatial and temporal properties of this SOBI component indicate that SOBI can extract task related neuronal signals originating from visual cortex despite continuous free-eye movement throughout the task

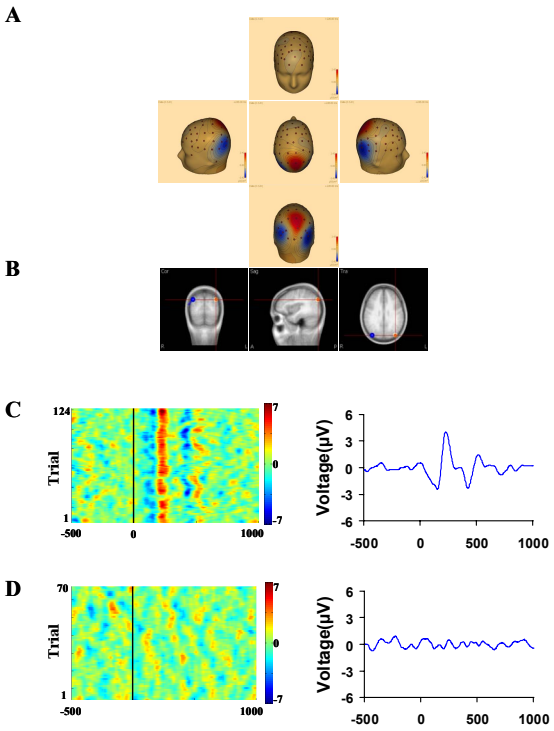


Fig. 5. A SOBI-recovered visual component. Arranged as in Figure 4.

and despite a lack of discretely presented visual stimuli. Notice that this VEP (Fig. 5C) and the activity associated with lateral eye movements (Fig. 4C) are temporally overlapping. Therefore, SOBI can extract VEPs from visual processing areas of the brain even when such VEPs were consistently preceded by a large eye movement. (For discussion of Fig. 5D please see Section E).

Furthermore, this visual component was reliably isolated from each of the three subjects assessed (Fig. 6). The averaged evoked potentials from each subject resembled a VEP recorded under ideal experimental conditions. The peak latencies of these components are around 200 ms, later than the latency of the expected N100 peak, typically associated with visual stimulation. Such a delay is expected because time zero corresponds to the pressing of the COMM button and at such time the subjects' eyes are fixed at the COMM button location. Following the COMM button press, the subject must first make a horizontal eye movement to the text box before reading the displayed text. We speculate that this visual ERP reflected activity associated with the processing of the text in the message display box. The lack of activity in the ERPs locked to the WARN events, which require only a 3-sec wait period, appears to confirm this speculation.

### *D. Isolation of Neuronal Activity Related to Executive Monitoring*

As would be expected for any task requiring the use of sensory information for complex decision making, the executive part of the brain must somehow gain access to the

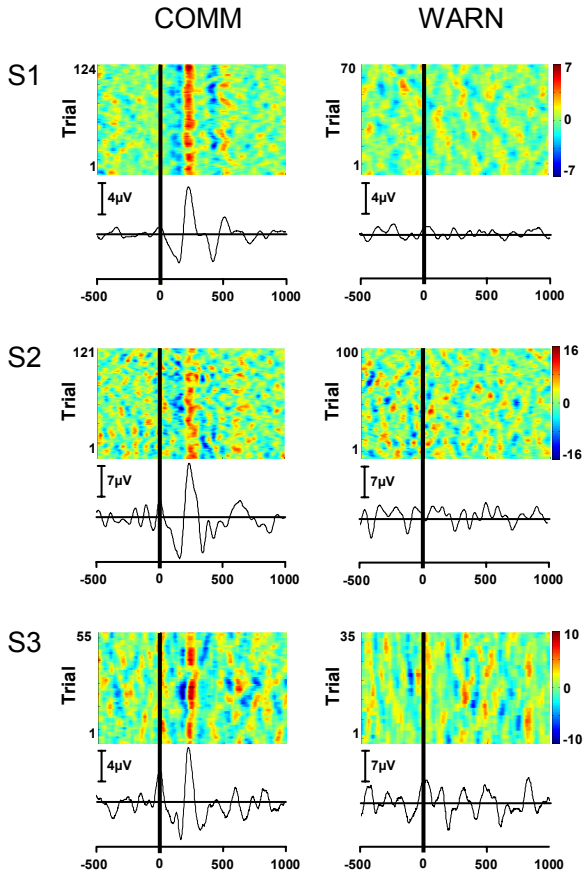


Fig 6. Visual components from each of the three subjects time-locked to COMM and WARN events.

sensory information. Synchronized activation between the frontal and posterior sensory areas has been suggested to mediate this sensory-motor integration. We were able to extract SOBI components that corresponded to synchronized anterior and posterior neuronal sources of activation (SAP) as indicated by the CSD maps (Fig. 7A). These components can be fit by two pairs of symmetric dipoles that are localized to both the frontal and posterior parietal lobes with >90% goodness-of-fit (Fig. 7B). The COMM event-triggered single-trial and average waveforms (Fig. 7C) showed clear evoked potentials that may reflect activity associated with executive function. (For discussion of Fig. 7D please see section E). Similar to the visual component, this component can also be isolated in all three subjects but differed from the visual component in that the ERP waveforms were more variable across subjects (data not shown).

### *E. ERPs for Events of High and Low Processing Load*

One feature of the task under study is that the information processing load can change from moment-to-moment during the task. Numerous events occur during the task and the low and high "processing load" events (WARN and COMM,

respectively) are intermixed. To examine whether the activity of V and SAP SOBI-recovered components captured

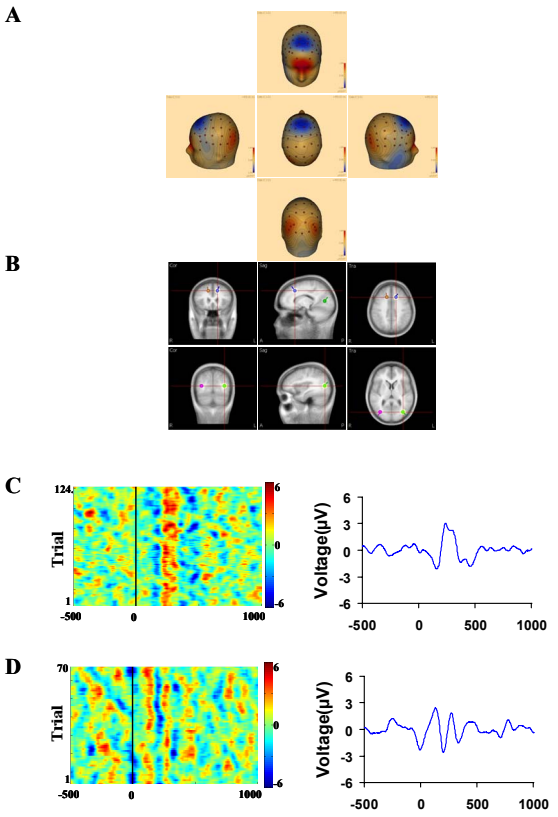


Fig. 7. A SOBI-recovered synchronized anterior-posterior (SAP) component. Arranged as in Figure 4.

these moment-to-moment differences in processing load, we contrasted "single-trial" ERP displays from the WARN and COMM events. The V component showed clear discrimination between the COMM and WARN events (compare Fig. 5C and 5D). Interestingly, even though visual information continues to be delivered during the simple action of pressing the WARN button, little activity over posterior scalp regions was observed (Fig. 5D). This contrasts sharply with the clear visual evoked responses observed after the COMM button press, after which the operator must read some text. The SAP component also showed temporally distinct ERPs between the COMM and WARN events (compare Fig. 7C and 7D). This is consistent with the expected difference in executive function when one is preparing for a firing action versus when one is processing language information.

### *F. Classification*

The contrasting component ERP waveforms between the WARN and COMM events suggest that one may be able to determine from a single-trial whether the operator is experiencing, at that moment, low or high information processing load. To test this hypothesis, we trained neural networks to classify the single-trial ERPs of the V and SAP

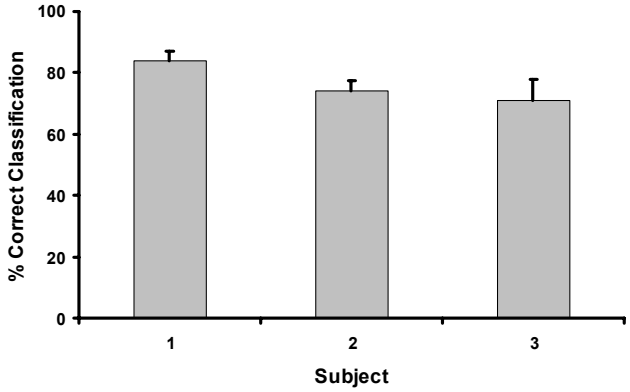


Fig 8. Classification of COMM and WARN events using the V and SAP SOBI-recovered components. Error bars are standard deviations.

components[1] into two classes: the high versus low demand events (corresponding to the COMM and WARN events). Figure 8 shows that after training the networks to the 95% correct classification criterion on the training data set, these networks classified the testing set with 84%, 74% and 71% accuracy, respectively for the three subjects. Note that further improvement in classification accuracy may be achieved by optimizing various network related parameters or using other classification algorithms.

## IV. Conclusions

We presented empirical data that demonstrate significant advances in the capability of human EEG signal processing. First, information processing-related signals from the human brain, as measured by ERPs, were obtained in the presence of continuous and varying ocular artifacts. Second, the spatial origins of such ERPs were estimated, hence providing critical information for a more precise interpretation of such ERPs than conventional ERPs measured at the scalp. Third, an improved effective signal-to-noise ratio allowed for the measurement of ERPs associated with the processing of single-events (i.e. single-trial ERPs). The validity of such ERPs is supported by the demonstration that events requiring high and low cognitive processing load can be classified using these single-trial ERPs. We expect further improvement in the classification accuracy when more recently developed classifiers, such as support vector machines, are used.

## References

[1] T.W. Picton, S. Bentin, P. Berg, E. Donchin, S.A. Hillyard, R. Johnson Jr., G.A. Miller, W. Ritter, D.S. Ruchkin, M.D. Rugg, and M.J. Taylor, "Guidelines for using human event-related potentials to study congnition: Recording standards and publication criteria," *Psychophysiol.* Vol. 37, pp. 127-152, 2000.

[1] The ocular component was not used for classification because the horizontal eye moment happens to precede the high load events (COMM).

[2] A. Hyvarinen, and E. Oja, "Independent component analysis: Algorithms and applications," *Neural Networks,* vol. 13, pp. 411-430, 2000.
[3] R.N. Vigario, J. Sarela, V. Jousmaki, M. Hamalainen, and E. Oja, "Independent component approach to the analysis of EEG and MEG recordings," *IEEE Trans. Biomed. Eng.*, vol. 47, pp. 589-593, 2000.
[4] J.V. Stone, "Independent component analysis: An introduction," *Trends in Cogn. Sci.*, vol. 6, pp. 59-64, 2002.
[5] S. Makeig, S. Debener, J. Onton, and A. Delorme, "Mining event-related brain dynamics," *Trends in Cogn. Sci.*, vol. 8, no. 5, pp.204-210, 2004.
[6] K.R. Muller, R. Vigario, F. Meinecke, and A. Ziehe, "Blind source separation techniques for decomposing event-related brain signals," *Int. J. Bifurc. Chaos*, vol. 14, pp. 773-791, 2004.
[7] R.N. Vigario, "Extraction of ocular artifacts from EEG using independent component analysis," *Electroenceph. and Clin. Neurophysiol.,* vol. 103, pp. 395-404, 1997.
[8] T.-P. Jung, C. Humphries, T.-W. Lee, M.J. McKeown, V. Iragui, S. Makeig, and T.J. Sejnowski, "Removing electroencephalographic artifacts by blind source separation," *Psychophysiol.*, vol. 37, pp. 163-178, 2000.
[9] A.C. Tang, B.A. Pearlmutter, N.A. Malaszenko, D.B. Phung, and B.C. Reeb, "Independent components of magnetoencephalography: Localization," *Neural Computation*, vol. 14, pp. 1827-1858, 2002.
[10] A.C. Tang, M.T. Sutherland, and C.J. McKinney, "Validation of SOBI-components from high-density EEG," *NeuroImage*, vol. 25, pp. 539-553, 2005.
[11] C.A. Joyce, I.F. Gorodnitsky, and M. Kutas, "Automatic removal of eye movement and blink artifacts from EEG using blind component separation," *Psychophysiol.*, vol. 41, pp. 313-325, 2004.
[12] A. Belouchrani, K. Abed-Meraim, J.-F. Cardoso, E. Moulines, "A blind source separation technique using second-order statistics," *IEEE. Trans. on Signal Processing,* vol. 45, no. 2, pp. 434-444, Feb. 1997.
[13] A.C. Tang, J.-Y. Liu, and M.T. Sutherland, "Recovery of correlated neuronal sources from EEG: The good and bad ways of using SOBI," *NeuroImage*, vol. 28, pp. 507-519, 2005.
[14] A.C. Tang, B.A. Pearlmutter, M. Zibulevsky, S.A. Carter, "Blind source separation of multichannel neuromagnetic responses," *Neurocomputing*, vol. 32, pp. 1115-1120, 2000.
[15] A.C. Tang, B.A. Pearlmutter, N.A. Malaszenko, and D.D. Phung, "Independent components of magnetoencephalography: Single-trial response onset times," *NeuroImage*, vol. 17, pp. 1773-1789, 2002.
[16] A.C. Tang, M.T. Sutherland, and Y. Wang, "Contrasting single-trial ERPs between experimental manipulations: Improving differentiability by blind source separation," *NeuroImage*, vol. 29, pp.335-346, 2006.
[17] M. St. John, D.A. Kobus, and J.G. Morrison, "A multi-tasking environment for manipulating neural correlates of cognitive workload," in Proceedings of the IEEE 7th Conference on Human Factors and Power Plants, 2002.
[18] J.-F. Cardoso, and A. Souloumiac, "Jacobi angles for simultaneous diagonalization," SIAM J. of Matrix Analysis and Applications, vol. 17, no.1, pp.161-164, Jan. 1996.
[19] T.D. Langerlund, "EEG source localization (model-delendent and model-independent methods)," in *Electroencephalography: Basic Principles, Clinical Applications, and Related Fields*, E. Neidermyer, and L. Da Silva, Eds. Baltimore: Lippincott, Williams, and Wilkins, 1999, pp. 809-822.
[20] M. Scherg, "Fundamentals of dipole source potential analysis," in *Advances in Audiology*, F. Grandori, M. Hoke, G.L. Romani, Eds. Basel: Krager, 1990, pp. 40-69.
[21] H. Hamalainen, R. Hari, R.J. Ilmoniemi, J. Knuutila, and O.V. Lounasmaa, "Magnetoencephalography: Theory instrumentation, and applications to noninvasive studies of the working human brain," *Rev. Modern Physics*, vol. 65, pp. 413-497, 1993.
[22] J. Sarvas, "Basic mathematical and electromagnetic concepts of the biomagnetic inverse problem," *Pys. Med. Biol.*, vol. 32, pp. 11-22, 1987.
[23] A.A. Ioannides, J.P.R. Bolton, and C.J.S. Clark, "Continuous probabilistic solutions to the biomagnetic inverse problem," *Inverse Problem*, vol. 6, pp. 523-542, 1990.
[24] M.T. Hagan, H.B. Demuth, and M.H. Beale, *Neural Network Design*, Boston, MA, PWS Publishing, 1996.